(P)GaCl; i.e., the spectra had a B(1,0) band and a Soret band shifted towards lower wavelengths. This is illustrated in Figure 9 for the case of (TPP)Ga(CH_3). Oxidation of all the tetraphenyl derivatives led to the same final species with a Soret peak at 423 nm and Q bands at 554 and 595 nm. Oxidation of the octaethyl derivatives also led to the same final species, which has a Soret band at 387 nm and Q bands at 534 and 572 nm. These spectra can reasonably be attributed to the corresponding (P)Ga(PF_6) complexes.

Comparison of (P)Ga(R) Reactivity with That of Other (P)M(R) Complexes. The reduction of organocobalt complexes leads to a cleavage of the cobalt-carbon bond.[49] In contrast, the addition of electrons to (P)In(R)[36] or (P)Ga(R) generates relatively stable singly and doubly reduced species. A stable anionic complex is also generated upon reduction of (P)Fe(C_6H_5),[50-52] but the reduction of iron porphyrin complexes with σ-bonded R groups such as C_6F_5 or C_6F_4H leads to rapid cleavage of the iron-carbon bond.[53] These differences in stability may result from differences in the site of electron transfer. The addition of an electron to the organocobalt complex and to (P)Fe(C_6F_5) involves reduction at the orbitals of the metal ion. This is not the case for (P)Ga(R) or (P)In(R), where anion radicals and dianions are formed. There is very little interaction of the σ-bonded ligand with the negatively charged conjugated π ring system, and this is reflected in the lack of substituent effects on the reduction potentials of (TPP)Ga(R) and (OEP)Ga(R).

It is also interesting to compare the chemical reactivity of singly oxidized $[(P)Ga(R)]^+$ with that of singly oxidized $[(P)In(R)]^+$, $[(P)Fe(R)]^+$, and $[(P)Co(R)]^+$. All three compounds are highly unstable, and after electrochemical generation from the corresponding $(P)M^{III}(R)$ derivative, each compound undergoes a rapid cleavage of metal-carbon bond.[15,36,51,52] They differ, however, in that both the iron and the cobalt derivatives undergo a metal to nitrogen migration resulting in the corresponding *N*-alkylporphyrin with an M(II) center. This migration does not occur during decomposition of $[(P)In(R)]^+$ or $[(P)Ga(R)]^+$, presumably due to the lack of an In(II) or Ga(II) oxidation state, which would be needed for the indium and gallium *N*-alkylporphyrin. In fact, to our knowledge, no indium or gallium *N*-alkylporphyrins have ever been synthesized.

Acknowledgment. The support of the National Science Foundation (Grant 8215507) is gratefully acknowledged. Discussions with Jean-Luc Cornillion regarding the (TPP)GaX and (OEP)GaX complexes are gratefully appreciated.

Registry No. (TPP)Ga($C(CH_3)_3$), 98943-15-8; (TPP)Ga($C(CH_3)_3$)$^+$, 98943-37-4; (TPP)Ga($C(CH_3)_3$)$^-$, 98943-23-8; (TPP)Ga(C_4H_9), 87607-78-1; (TPP)Ga(C_4H_9)$^+$, 98943-38-5; (TPP)Ga(C_4H_9)$^-$, 98943-24-9; (TPP)Ga(C_2H_5), 87607-77-0; (TPP)Ga(C_2H_5)$^+$, 98943-39-6; (TPP)Ga(C_2H_5)$^-$, 98943-25-0; (TPP)Ga(CH_3), 87607-76-9; (TPP)Ga(CH_3)$^+$, 98943-40-9; (TPP)Ga(CH_3)$^-$, 98943-26-1; (TPP)Ga($C_2H_2C_6H_5$), 98943-16-9; (TPP)Ga($C_2H_2C_6H_5$)$^+$, 98943-41-0; (TPP)Ga($C_2H_2C_6H_5$)$^-$, 98943-27-2; (TPP)Ga(C_6H_5), 87607-79-2; (TPP)Ga(C_6H_5)$^+$, 98943-42-1; (TPP)Ga(C_6H_5)$^-$, 98943-28-3; (TPP)Ga($C_2C_6H_5$), 98943-17-0; (TPP)Ga($C_2C_6H_5$)$^+$, 98943-43-2; (TPP)Ga($C_2C_6H_5$)$^-$, 98943-29-4; (TPP)GaCl, 78833-52-0; (TPP)GaCl$^+$, 98943-44-3; (TPP)GaCl$^-$, 98943-21-6; (TPP)Ga(*p*-MeC_6H_4), 87607-80-5; (OEP)Ga($C(CH_3)_3$), 98943-18-1; (OEP)Ga($C(CH_3)_3$)$^+$, 98943-45-4; (OEP)Ga($C(CH_3)_3$)$^-$, 98943-30-7; (OEP)Ga(C_4H_9), 87607-73-6; (OEP)Ga(C_4H_9)$^+$, 98943-46-5; (OEP)Ga(C_4H_9)$^-$, 98943-31-8; (OEP)Ga(C_2H_5), 87607-72-5; (OEP)Ga(C_2H_5)$^+$, 98943-47-6; (OEP)Ga(C_2H_5)$^-$, 98943-32-9; (OEP)Ga(CH_3), 87607-71-4; (OEP)Ga(CH_3)$^+$, 98943-48-7; (OEP)Ga(CH_3)$^-$, 98943-33-0; (OEP)Ga($C_2H_2C_6H_5$), 98943-19-2; (OEP)Ga($C_2H_2C_6H_5$)$^+$, 98943-49-8; (OEP)Ga($C_2H_2C_6H_5$)$^-$, 98943-34-1; (OEP)Ga(C_6H_5), 87607-74-7; (OEP)Ga(C_6H_5)$^+$, 98943-50-1; (OEP)Ga(C_6H_5)$^-$, 98943-35-2; (OEP)Ga($C_2C_6H_5$), 98943-20-5; (OEP)Ga($C_2C_6H_5$)$^+$, 98943-51-2; (OEP)Ga($C_2C_6H_5$)$^-$, 98943-36-3; (OEP)GaCl, 87607-70-3; (OEP)GaCl$^+$, 98943-52-3; (OEP)GaCl$^-$, 98943-22-7; (OEP)Ga(*p*-MeC_6H_4), 87607-75-8; TBA(PF_6), 3109-63-5.

(49) Lexa, D.; Saveant, J. M. *Acc. Chem. Res.* **1983**, *16*, 235.
(50) Lexa, D.; Saveant, J. M. *J. Am. Chem. Soc.* **1982**, *104*, 3503.
(51) Lancon, D.; Cocolios, P.; Guilard, R.; Kadish, K. M. *J. Am. Chem. Soc.* **1984**, *106*, 5724.
(52) Lancon, D.; Cocolios, P.; Guilard, R.; Kadish, K. M. *Organometallics*, **1984**, *3*, 1164.
(53) Guilard, R.; Boisselier-Cocolios, B.; Tabard, A.; Cocolios, P.; Simonet, B.; Kadish, K. M. *Inorg. Chem.* **1985**, *24*, 2509.

Contribution from the Department of Inorganic Chemistry, Indian Association for the Cultivation of Science, Calcutta 700032, India

Binding of a Nickel(IV) Complex to a Polyion-Modified Graphite Electrode: Electroprotic Equilibria

Rabindranath Mukherjee, Sreebrata Goswami, and Animesh Chakravorty*

Received December 17, 1984

The cationic $Ni^{IV}N_6$ complex, NiL^{2+}, of the hexadentate dioxime ligand (MeC(=NOH)C(Me)=$NCH_2CH_2NHCH_2$-)$_2$ (H_2L) has been incorporated by ion-exchange forces into poly(*p*-styrenesulfonate) (P-SS) films attached to a basal pyrolytic graphite (bpg) electrode surface over the pH range 1-9. Optimal binding is achieved in acidic solution (pH 3-5). The variable-pH cyclic voltammetry of the surface-bound complex has revealed that at pH <5 the single 2e-2H^+ couple $Ni^{IV}L^{2+}/Ni^{II}(H_2L)^{2+}$ (formal potential, $E^{\circ\prime}_{298}$, 0.72 ± 0.01 V) is operative. At alkaline pH, two 1e couples become observable: $Ni^{IV}L^{2+}/Ni^{III}L^+$ (0.42 ± 0.01 V) followed by $Ni^{III}L^+/Ni^{II}(HL)^+$ (0.66 ± 0.01 V; pH <8.5) or $Ni^{III}L^+/Ni^{II}L$ (0.17 ± 0.01 V; pH ≥8.5). This pattern of electroprotic equilibria is virtually the same as that observed for homogeneous aqueous solutions of NiL^{2+} at a bare bpg electrode. The cyclic voltammetric peak current of the surface-confined species (pH 4.05; 298 K) varies as the square root of scan rate over a wide range of surface coverage. The charge transport rate is thus slow, the diffusion coefficient being of the order of 10^{-9} cm^2/s. The equilibrium ratio of the concentration of NiL^{2+} in the polymer film to that in the loading solution is 30 ± 10 at 298 K and pH 4.05. The loss of incorporated NiL^{2+} from the loaded electrode into the buffer solution follows first-order kinetics with a rate constant of (3.5 ± 0.5) × 10^{-4} s^{-1} under the same conditions. In alkaline media such loss occurs at a higher rate on redox cycling presumably due to a diminution of ion-pair bond energy on reduction.

Introduction

The hexadentate amine-imine-oxime ligand[1] H_2L (**1**) and the conjugate oximato bases HL^- and L^{2-} display remarkable affinity for nickel and afford[2-4] pseudooctahedral NiN_6 species (**2**) spanning the oxidation states +2, +3 and +4. The structures of $[Ni^{IV}L](ClO_4)_2$ and $[Ni^{II}(H_2L)](ClO_4)_2$ are accurately known

(1) Ablov, A. V.; Belichuk, N. I.; Kaftanat, V. N. *Russ. J. Inorg. Chem. (Engl. Transl.)* **1972**, *17*, 392.
(2) Mohanty, J. G.; Chakravorty, A. *Indian J. Chem.* **1974**, *12*, 883. Mohanty, J. G.; Singh, R. P.; Chakravorty, A. *Inorg. Chem.* **1975**, *14*, 2178.
(3) Mohanty, J. G.; Chakravorty, A. *Inorg. Chim. Acta* **1976**, *18*, L33. Mohanty, J. G.; Chakravorty, A. *Inorg. Chem.* **1976**, *15*, 2912.

0020-1669/85/1324-4528$01.50/0

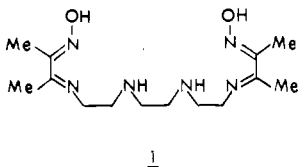

1

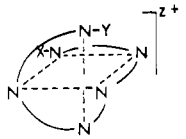

	X	Y	z
Ni^{II}	OH	OH	2
	OH	O	1
	O	O	0
Ni^{III}	OH	O	2
	O	O	1
Ni^{IV}	O	O	2

2

from X-ray work.[5-7] Violet $[NiL](ClO_4)_2$ is a potent outer-sphere oxidant.[8,9] The accessibility of three metal oxidation states and three levels of ligand protonation make the nickel complexes ideally suited for the display of an array of electroprotic equilibria in aqueous solution as revealed by variable-pH voltammetry.[3,10,11]

This work stems from our interest in learning the nature of such equilibria when the nickel species get bound to the surface of a suitably modified electrode. Polyelectrolytes spontaneously trap counterions[12,13] by electrovalent forces, and they also attach well to surfaces. Recently these properties have been used[14-16] to develop polyelectrolyte-coated electrodes for surface binding of electroactive complex ions. We have explored this approach for the attachment of NiL^{2+} to electrodes.

Results and Discussion

A. Voltammetry at a Bare Electrode. We have used polyelectrolyte-coated basal pyrolytic graphite (bpg) for the surface binding of NiL^{2+}. It is therefore necessary to ascertain the electroprotic behavior of the complex at a bare bpg electrode first. This behavior is found to be closely similar[17] to that at platinum, which was used as the electrode material in all reported works.[3,10,11] A cyclic voltammogram at a bare bpg electrode is shown in Figure 1 and variable-pH formal potential ($E^{\circ\prime}_{298}$) data are collected in Table I. All potentials are referenced to the saturated calomel electrode (SCE).

Table I. Variable-pH Electrochemical Data[a,b] of Solution and P-SS-Bound NiL^{2+} at a Basal Pyrolytic Graphite Electrode at 298 K

pH	couple	$\bar{E}_p$,[c] V	$E^{\circ\prime}_{298}$,[d] V	$10^9\Gamma_{Ni}$, mol/cm^2
	(A) NiL^{2+} Solution at Bare Electrode[e,f]			
1.31	3	0.64	0.72	
3.02	3	0.54	0.72	
4.05	3	0.48	0.72	
6.34	1, 2b	0.42, 0.29	0.42, 0.66	
7.29	1, 2b	0.41, 0.22	0.41, 0.65	
9.00	1, 2a	0.42, 0.17	0.42, 0.17	
	(B) Incorporated NiL^{2+}[g,h]			
1.54	3	0.64	0.73	3.0
2.56	3	0.58	0.73	3.8
3.05	3	0.55	0.73	4.1
4.05	3	0.47	0.71	5.0
7.29	1, 2b	0.41, 0.24	0.41, 0.67	2.4
7.79	1, 2b	0.42, 0.20	0.42, 0.66	1.2
8.35	1, 2b	0.41, 0.17	0.41, 0.66	1.1
8.50	1, 2a	0.41, 0.18	0.41, 0.18	1.0
9.00	1, 2a	0.41, 0.17	0.41, 0.17	*i*

[a] Potentials are vs. SCE. [b] Scan rate 0.02 V/s. [c] $\bar{E}_p$ is the average of cathodic and anodic peak potentials. [d] Calculated from the relationship $E^{\circ\prime}_{298} = \bar{E}_p + 0.059\ (m/n)$pH where m and n are respectively the number of protons and electrons transferred. The formal potentials are reproducible to within ±0.01 V. [e] Solute concentration $\sim 10^{-3}$ M. [f] The peak-to-peak separation (ΔE_p) values are as follows: couple 3, 40–70 mV; couple 1, 70–95 mV; couple 2b, 65–80 mV; couple 2a, 90–115 mV. [g] Loading solution concentration range, (1.01–1.50) × 10^{-3} M; quantity of P-SS introduced per unit area of the electrode surface, 1.2×10^{-6} mol/cm^2 (expressed as monomer). [h] The ΔE_p values are as follows: couple 3, 20–40 mV; couple 1, 60–80 mV; couple 2b, 70–120 mV; couple 2a, 85–100 mV. [i] Coverage too low for accurate determination.

At high pH (≥8.5) the successive proton-independent couples 1 and 2a are observed. When the pH is lowered, protonation[18] of NiL occurs and couple 2a is progressively replaced by couples

$$Ni^{IV}L^{2+} + e^- \rightleftharpoons Ni^{III}L^+ \quad (1)$$

$$Ni^{III}L^+ + e^- \rightleftharpoons Ni^{II}L \quad (2a)$$

$$Ni^{III}L^+ + e^- + H^+ \rightleftharpoons Ni^{II}(HL)^+ \quad (2b)$$

$$Ni^{III}L^+ + e^- + 2H^+ \rightleftharpoons Ni^{II}(H_2L)^{2+} \quad (2c)$$

$$Ni^{IV}L^{2+} + 2e^- + 2H^+ \rightleftharpoons Ni^{II}(H_2L)^{2+} \quad (3)$$

2b (pH 6–8) and 2c.[19,20] As a result the peak potential of the nickel(III)–nickel(II) couple approaches that of the nickel(IV)–nickel(III) couple with diminishing pH. The two couples become equipotential at pH ~5, and below this pH the single nickel(IV)–nickel(II) couple 3 is all that remains observable.[21,22]

B. Electrode Modification and Surface Incorporation of NiL^{2+}. The anionic polyelectrolyte used in the present work is poly(*p*-styrenesulfonate) (P-SS), which is known to attach well to bpg[15] and platinum[23] surfaces. The efficacy of P-SS films on bpg[15] and of related copolymer films on platinum[24] in surface binding of

(4) Nag, K.; Chakravorty, A. *Coord. Chem. Rev.* **1980**, *33*, 87. Chakravorty, A. *Isr. J. Chem.* **1985**, *25*, 99.
(5) Korvenranta, J.; Saarinen, H.; Nasakkala, M. *Inorg. Chem.* **1982**, *21*, 4296.
(6) Some information on $[Ni^{III}(HL)](ClO_4)_2$ is also available.[7]
(7) McAuley, A.; Preston, K. F. *Inorg. Chem.* **1983**, *22*, 2111.
(8) Munn, S. F.; Lannon, A. M.; Laranjeira, M. C. M.; Lappin, A. G. *J. Chem. Soc., Dalton Trans.* **1984**, 1371. Lappin, A. G.; Laranjeira, M. C. M.; Peacock, R. D. *Inorg. Chem.* **1983**, *22*, 786. Lappin, A. G.; Laranjeira, M. C. M.; Youde-Owei, L. *J. Chem. Soc., Dalton Trans.* **1981**, 721. Allan, A. E.; Lappin, A. G.; Laranjeira, M. C. M. *Inorg. Chem.* **1984**, *23*, 477.
(9) Macartney, D. H.; McAuley, A. *J. Chem. Soc., Dalton Trans.* **1984**, 103. Macartney, D. H.; McAuley, A. *Inorg. Chem.* **1983**, *22*, 2062. Macartney, D. H.; Sutin, N. *Inorg. Chem.* **1983**, *22*, 3530.
(10) Lappin, A. G.; Laranjeira, M. C. M. *J. Chem. Soc., Dalton Trans.* **1982**, 1861.
(11) Macartney, D. H.; McAuley, A. *Can. J. Chem.* **1983**, *61*, 103.
(12) Breuer, M. M. In "Polymer Science"; Jenkins, A. D., Ed.; North-Holland Publishing Company: Amsterdam and London, 1972; Vol. 2, pp 1135–1185.
(13) Rice, S. A.; Nagasawa, M. "Polyelectrolyte Solutions"; Academic Press: London and New York, 1961; pp 427–495.
(14) Oyama, N.; Anson, F. C. *J. Electrochem. Soc.* **1980**, *127*, 247. Rubinstein, I.; Bard, A. J. *J. Am. Chem. Soc.* **1980**, *102*, 6641.
(15) Oyama, N.; Shimomura, T.; Shigehara, K.; Anson, F. C. *J. Electroanal. Chem. Interfacial Electrochem.* **1980**, *112*, 271.
(16) Oyama, N.; Ohsaka, T.; Kaneko, M.; Sato, K.; Matsuda, H. *J. Am. Chem. Soc.* **1983**, *105*, 6003. Oyama, N.; Anson, F. C. *J. Electrochem. Soc.* **1980**, *127*, 640.
(17) The electrochemical reversibility of the couples are poorer at the bpg electrode. Observed cyclic voltammetric peak-to-peak separation values for the 1e and 2e couples lie in the range 60–120 and 40–70 mV respectively (Table I) while in the case of platinum electrode the values approach the Nernstian situation.[3] The formal potentials at the bpg electrode lie within 20 mV of those[3] at platinum.
(18) The pK values of the various species are as follows:[3,10] $Ni(H_2L)^{2+}$, 5.90; $Ni(HL)^+$, 7.80; $Ni(HL)^{2+}$, 4.05; $Ni(HL)^{3+}$, <1.
(19) Direct experimental characterization of couple 2c has not been possible due to the lack of availability of a pH range where this couple alone contributes. However, from the principle of additivity[20] of free energy changes due to electron transfer and proton transfer, the formal potential of this couple is computed to be ~1.0 V on the basis of the E°_{298} of couple 2a and pK_1 and pK_2 values of $Ni(H_2L)^{2+}$.
(20) Mohanty, J. G.; Chakravorty, A. *Inorg. Chem.* **1977**, *15*, 1561.
(21) In chemical terms we have[22] here the situation where the nickel(III) complex spontaneously disproportionates to the corresponding nickel(II) and nickel(IV) species.
(22) Chakravorty, A. *Comments Inorg. Chem.* **1985**, *4*, 1.
(23) Kawaguchi, M.; Hayashi, K.; Takahashi, A. *Macromolecules* **1984**, *17*, 2066.
(24) Schneider, J. R.; Murray, R. W. *Anal. Chem.* **1982**, *54*, 1508.

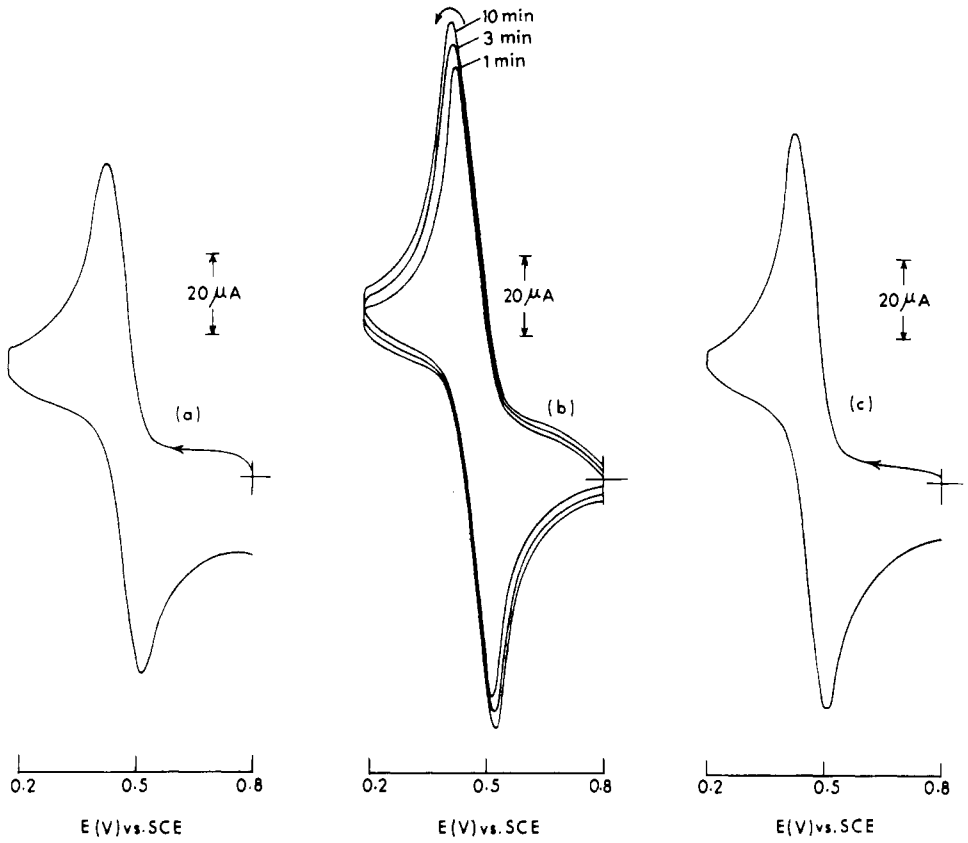

Figure 1. Cyclic voltammograms at a bpg electrode: (a) uncoated electrode in NiL^{2+} solution; (b) coated electrode (1.20×10^{-6} mol/cm^2 of P-SSH) in NiL^{2+} solution as a function of time after dipping; (c) coated electrode (1.43×10^{-7} mol/cm^2 of P-SSH) in NiL^{2+} solution after dipping for 10 min. In all cases the solution pH is 4.05 and the scan rate is 0.2 V/s.

complex cations like $Ru(NH_3)_6^{3+}$ and $Co(bpy)_3^{3+}$ has been documented.

We synthesized P-SS in the protonated form by polymerizing styrene into a polymer of average molecular weight 1.05×10^5 and then sulfonating the latter. A sulfonic acid group in the para position of each benzene ring is present in 70% of the cases. The apparent pK of the acid is[25] 1.95 ± 0.05. A freshly cut bpg electrode (area ~ 0.09 cm^2) was coated with the polymer either by dipping the electrode into polymer solution or by transferring a measured volume of polymer solution to the electrode surface. After solvent evaporation the complex was incorporated into the coating by dipping the electrode in a buffered solution of NiL^{2+} (loading solution). The electrochemical response[26] of the washed and dried loaded electrode bathed in a buffer solution free of NiL^{2+} but having the same pH as the loading solution was then investigated as a function of various parameters.

Leaving the effect of pH variation to a later section, we consider first the results obtained in acetate buffer of pH 4.05 to illustrate the main conclusions. The choice of pH $\sim$4 for detailed reporting is made because of the good loading and retention of NiL^{2+} in P-SS films and because of the sharpness of the observed voltammograms at such pH. In Figure 1 are shown metal-centered cyclic voltammetric responses at (a) an uncoated electrode dipped into a buffered NiL^{2+} solution, (b) a P-SS-coated electrode dipped as in part a, and (c) a P-SS-coated electrode as in (b) but with a thinner coat[27] of polymer. Since the pH is 4.05, the response in part a is due to couple 3 as stated earlier. In case b the response remains nearly unchanged in shape and form but has an augmented height, which increases[28] further with time due to progressive NiL^{2+} incorporation into the polyion.

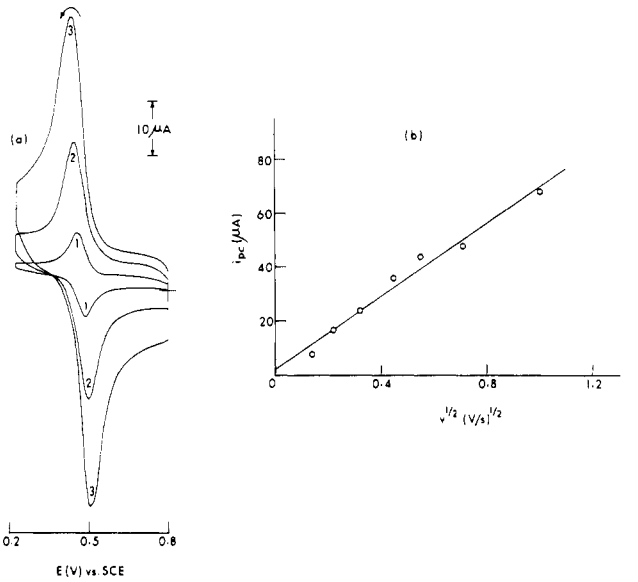

Figure 2. (a) Cyclic voltammograms of incorporated NiL^{2+} (buffer pH 4.05; Γ_{Ni}, 6.0×10^{-9} mol/cm^2) as a function of scan rate (v): (1) 0.02, (2) 0.1, (3) 0.3 V/s. (b) Least-squares plot of cathodic peak current (i_{pc}) against $v^{1/2}$ in the range v = 0.02–1 V/s.

(25) There is good evidence that polysulfonic acids are completely dissociated. The apparent dissociation constant corresponds to the partial localization of dissociated hydrogen ions by the strong electrostatic field of the polyanion.[13]

(26) That this response is due to genuine incorporation into P-SS and not due to adsorption on bpg was established by the failure of bare bpg to get loaded when dipped into NiL^{2+} solution.

(27) The general nature of the cyclic voltammetric response (Figure 1b,c) remains unchanged irrespective of the amount of polymer present per unit area of the surface within the range (1.20×10^{-6} to 1.43×10^{-8} mol/cm^2, expressed as monomer) employed in the present study.

(28) For full incorporation of $Ru(bpy)_3^{2+}$ etc into P-SS, repetitive potential cycling was used.[15] We have found this unnecessary, at least for NiL^{2+}. Full loading occurs by just keeping the polymer-coated electrode dipped into the loading solution.

Table II.[a,b] Surface Coverage and Distribution Coefficient Data for Incorporated NiL^{2+} at pH 4.05

$10^3[NiL^{2+}]$, M	$10^9\Gamma_{Ni}$, mol/cm^2	$10^5[NiL^{2+}]_p$, mol/L	K_d
1.01	5.00 ± 1.00	3000 ± 600	30 ± 6
0.11	0.58 ± 0.14	350 ± 80	32 ± 7
0.02	0.10 ± 0.03	60 ± 20	30 ± 10

[a] Meanings of symbols are as in the text. [b] Quantity of P-SS introduced per unit area of the electrode surface, 220 μg/cm^2.

In aqueous media containing Na^+ ion (our buffer solution is ~0.3 N in Na^+) polyion charge neutralization due to extensive ion-pair formation (site binding)[12,13,29-33] (eq 4) leads to loose

$$-SO_3^- + Na^+ \rightleftharpoons -SO_3^-,Na^+ \quad (4)$$

random coiling of the flexible P-SS chain. When polymer-coated bpg is bathed in an aqueous buffer, the polymer film is assumed to behave as an ensemble of the random coils, with each macroion having attachment at one or several points to the bpg surface. Addition of NiL^{2+} to the buffer leads to incorporation of electroactive cations into the polymer body by the ion-exchange equilibrium reaction 5, which is written in a way so as to hold

$$2(SO_3^-,Na^+) + NiL^{2+} \rightleftharpoons 2(-SO_3^-),NiL^{2+} + 2Na^+ \quad (5)$$

ion exchange charges in correct proportion. We shall return to eq 5 later in this work.

C. Voltammetry of Incorporated Complex. In Figure 2 is shown the variable-scan cyclic voltammogram of a loaded electrode dipped into pure buffer of pH 4.05. We are observing here couple 3 for the surface-confined complex. Since the formal potential is virtually the same as that of NiL^{2+} in homogeneous solution (Table I), we conclude that surface binding affects the state of NiL^{2+} only marginally. The amount of NiL^{2+} incorporated per unit area of the electrode surface (Γ_{Ni}, Table II) and surface concentration of the polymer[27] were each varied by nearly 2 orders of magnitude. Yet in all cases the peak currents (i_p) were found to vary linearly with $v^{1/2}$ (v = scan rate). One such case is illustrated in Figure 2. The separation (ΔE_p) between cathodic and anodic peak potentials were in the range 20–40 mV at low scan rates.

The nature of current–potential response of surface-confined species depends on the effective rate of electron propagation or charge transport to the electrode.[16,34-38] If transport is fast on the voltammetric time scale, symmetrical current–potential curves with $\Delta E_p \sim 0$ and i_p proportional to v result. In the limit of slow charge transport[35] the voltammograms develop tails on both cathodic and anodic halves, ΔE_p approaches or exceeds $59/n$ mV (n, the number of electrons transferred, equals 2 in couple 3) and i_p varies as $v^{1/2}$. In effect the Randles–Sevcik equation[39,40] becomes applicable but with a small diffusion coefficient.[35]

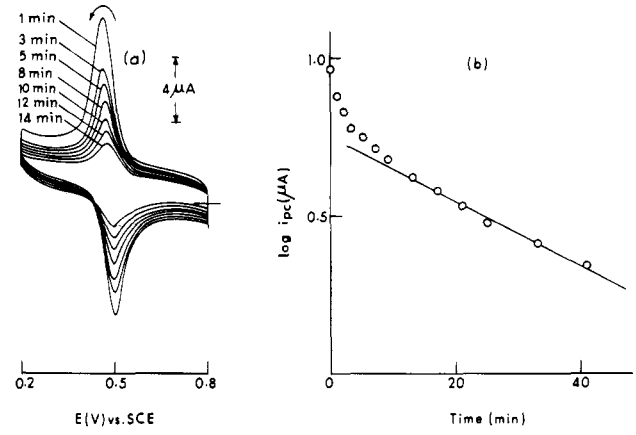

Figure 3. (a) Variable time cyclic voltammograms of a loaded electrode dipped into buffer pH 4.05 (scan rate 0.05 V/s). (b) Semilog plot of cathodic peak current (i_{pc}) vs. time. The Γ_{Ni} of the electrode at time = 0 is 5.0×10^{-9} mol/cm^2.

The voltammetric behavior of our loaded electrode agrees well with the slow charge transport condition. From the slope of the i_p–$v^{1/2}$ straight line of Figure 2, the order of magnitude of the diffusion coefficient (D) characterizing charge transport is estimated[41] to be 10^{-9} cm^2/s—a small but unexceptional[35] value. The motions of the P-SS segments that lead to fruitful electron-exchanging collisions (and hence charge transport) of electroactive centers are relatively infrequent. In couple 3 the oxidized and reduced complexes carry the same net charge due to the associated proton transfer. Since proton transfer in acidic aqueous media[42] is fast, a charge-compensating counterion motion[35,37] is unlikely to be rate controlling in the present case.

D. Distribution Coefficient and Ion-Loss Kinetics. Below the saturation level, the extent of NiL^{2+} incorporation (eq 5) into the polymer film at equilibrium should increase with increasing $[NiL^{2+}]$, the concentration of NiL^{2+} in the loading solution. The Γ_{Ni} values of Table II are consistent with this. The distribution coefficient K_d corresponding to reaction 5 is given by eq 6, where

$$K_d = [NiL^{2+}]_p/[NiL^{2+}] \quad (6)$$

$[NiL^{2+}]_p$ is the concentration of NiL^{2+} within the polymer film. The latter quantity could be estimated from Γ_{Ni}, the electrode area, and the volume of the polymer film (see Experimental Section). Representative K_d values are given in Table II. The agreement of K_d values for different Γ_{Ni} values is satisfactory. Since K_d is >1, the P-SS film is able to concentrate NiL^{2+} significantly via the ion-exchange incorporation process. Distribution coefficient data for ion-exchange reactions on surface-bound thin films are sparse in the literature.[24]

When the loaded electrode is allowed to stand in the buffer solution, the back-reaction in eq 5 occurs, leading to progressive loss of incorporated NiL^{2+}. This is revealed by the systematic decay of the cyclic voltammetric peak current, initially rapidly and then at a slower[43-46] rate (Figure 3). The second phase is

(29) Kato, M.; Nakagawa, T.; Akamatu, H. *Bull. Chem. Soc.* Jpn. **1960**, *33*, 322.
(30) Caillé, A.; Daoust, H. *J. Polymn. Sci., Polym. Symp.* **1974**, *No. 45*, 153–163.
(31) Mauritz, K. A.; Hora, C. J.; Hopfinger, A. J. In "Ions in Polymers"; Eisenberg, A., Ed.; American Chemical Society: Washington, DC, 1980; Adv. Chem. Ser. No. 187, pp 123–144.
(32) The solution (pH 4.05) has a proton concentration of only 10^{-4} N and hence ion-pair binding is dominated by Na^+ rather than H^+.
(33) Tanford, C. "Physical Chemistry of Macromolecules"; Wiley: New York and London, 1961; p 482.
(34) Kaufman, F. B.; Engler, E. M. *J. Am. Chem. Soc.* **1979**, *101*, 547.
(35) Daum, P.; Lenhard, J. R.; Rolison, D.; Murray, R. W. *J. Am. Chem. Soc.* **1980**, *102*, 4649.
(36) Murray, R. W. *Ann. Rev. Mater. Sci.* **1984**, *14*, 145. Nowak, R. J.; Schultz, F. A.; Umaña, M.; Lam, R.; Murray, R. W. *Anal. Chem.* **1980**, *52*, 315.
(37) Buttry, D. A.; Anson, F. C. *J. Am. Chem. Soc.* **1983**, *105*, 685. Shigehara, K.; Oyama, N.; Anson, F. C. *J. Am. Chem. Soc.* **1981**, *103*, 2552.
(38) Laviron, E. J. *J. Electroanal. Chem. Interfacial Electrochem.* **1980**, *112*, 1. Lane, R. F.; Hubbard, A. T. *J. Phys. Chem.* **1973**, *77*, 1401.
(39) The equation can be written[40] in the form $i_P = 2.72 \times 10^8 n^{3/2} A D^{1/2} v^{1/2} C$, where units are as follows: i_p, μA; A, cm^2; D, cm^2/s; v, V/s and C, mol/L.
(40) Adams, R. N. "Electrochemistry at Solid Electrodes"; Marcel Dekker: New York, 1969; pp 128–129.
(41) The Randles–Sevcik equation[39] is used with A = 0.094 cm^2 and $C \sim 3 \times 10^{-2}$ mol/L (see Table II, Column 3) along with the $i_p - v^{1/2}$ slope of 67.5 $\mu As^{1/2}/V^{1/2}$.
(42) The polymer itself is extensively hydrated at the sulfonic acid groups. This explains the high solubility of P-SS acid and salts in water (polystyrene is insoluble). In a theoretical study of Nafion[31] the formation free energies of the ion–dipole pairs SO_3^-,H_2O and Na^+,H_2O are estimated at −18.8 and −13.8 kcal/mol, respectively. On the average, four water molecules interact with each SO_3^- ion. The ion pairing energy of SO_3^-,Na^+ is −48.3 kcal/mol. In P-SS, the sulfonate functions occur at close intervals and therefore the hydration shells are also closely spaced along the polymer body, which thus has a sheath of solvation layer. The electroactive complex remains bound at sulfonate sites (eq 5). The configuration is thus appropriate for facile ingress and egress of protons.
(43) A phase of rapid initial loss followed by a slower phase appears to be a general characteristic of surface bound species.[44-46]

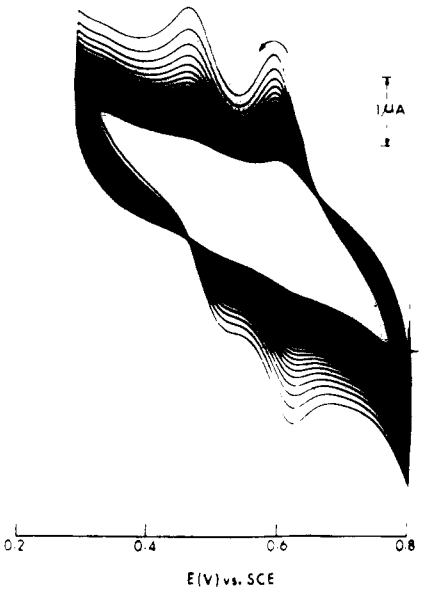

Figure 4. Repetitive scan cyclic voltammograms of incorporated NiL^{2+} at pH 8.35. Scan rate is 0.05 V/s, and total scanning time is approximately 30 min.

sufficiently prolonged to be characterized as a first-order process with a rate constant of $(3.5 \pm 0.5) \times 10^{-4}$ s^{-1} (298 K; pH 4.05). The half-life of incorporated NiL^{2+} under these conditions is approximately 30 min. Since Na^+ ions in eq 5 are present in large excess, the observed first-order dynamics of NiL^{2+} loss from the film is understandable.

Due to the strong hydrophilic nature[42] of P-SS, the possibility that it itself is leached out from the electrode surface, thus accounting for the loss of NiL^{2+}, must be considered. Polymer loss indeed occurs but at a relatively slow rate. This was established by first depleting NiL^{2+} from a loaded electrode by diffusion in buffer and then reloading the electrode without adding a new polymer coat. On such reloading 90% of the original current height could be recovered. The rate constant for polymer loss is estimated to be $\sim 10^{-5}$ s^{-1}.

E. Effect of pH Variation. It has been possible to incorporate NiL^{2+} into P-SS films over the pH range[47] 1–9. The electroprotic behavior of polymer-attached NiL^{2+} is entirely analogous to that of free NiL^{2+} at a bare bpg electrode over this pH range: Figure 4 and Table I. Below pH 5, couple 3 is observed and the peak potentials display the expected shift of ~60 mV/unit change of pH. Above pH 5, the voltammogram first broadens and then splits, leading to separate responses (couple 1 and 2b) clearly observable at pH >7. When pH 8.5 is reached, the relevant couples are couples 1 and 2a. The formal potentials of all couples of the incorporated species are *identical* with those of free NiL^{2+} within experimental error (Table I).

The analogous nature of the electroprotic behavior of free and P-SS-bound NiL^{2+} is significant and can be rationalized. The random coiling in P-SS is loose, and the polymer body remains relatively open and accessible to external solution (free-draining coils).[29,33] The polymer has a sheath of hydration layer.[42] Therefore the pH at the polymer-bound electroactive sites is essentially the same as that of the bulk solution, and unrestricted transfer of protons can occur[42] whenever required.

In general Γ_{Ni} values are larger in acidic pH as compared to values in alkaline pH (Table I). Loss of incorporated nickel species also occurs relatively rapidly on redox cycling at alkaline pH. This can be rationalized in terms of weaker binding of reduced species at such pH. In acidic solution (couple 3) the net positive charges on the oxidized and reduced complexes are the same. In alkaline media (eq 1, 2a) the reduced species have lower positive charges than those of their oxidized counterparts. The ion-pairing energy therefore decreases on reduction. The optimum pH range for incorporation and subsequent retention is 3–5.

F. Concluding Remarks. It is demonstrated that the nickel(IV) complex NiL^{2+} can be incorporated to varying degrees into P-SS films on a bpg electrode by ion-exchange forces over a wide range of pH. Best results are however obtained at pH 3–5. Distribution coefficient data for the ion-exchange equilibrium between bulk NiL^{2+} and incorporated NiL^{2+} in acidic solution show that the polymer film acts as a concentrator of the nickel(IV) cation. The electroprotic behavior of incorporated NiL^{2+} is closely similar to that of free NiL^{2+} at a bare bpg electrode. The pH within the polymer film is thus the same as that in bulk solution. The redox charge transport rate for NiL^{2+} bound to P-SS film is slow presumably due to the rarity of fruitful electron-exchanging collisions of loaded polymer segments.

The fast outer-sphere oxidation of a number of reducing agents by NiL^{2+} has been kinetically characterized in homogeneous solution.[8,9] We have explored the possible electrocatalysis[46] of such oxidations in the cases of Fe^{2+} and ascorbic acid with the help of NiL^{2+}-loaded electrodes at acidic pH. In both cases the oxidation wave of the reductant shifted to higher potential in going from bare to P-SS-coated bpg electrodes, but the shift was insufficient to make the potential higher than the peak potentials of NiL^{2+}. This has made effective demonstrations of electrocatalysis difficult. Further work on this problem is in progress.

Experimental Section

Chemicals. The nickel(IV) complex, $[NiL](ClO_4)_2$ was prepared in the usual manner.[3] Deionized water was used in all experiments. All chemicals used for the preparation of buffer were of reagent grade. Buffers were prepared from (i) sodium acetate and hydrochloric acid (pH 0.7–5.2), (ii) disodium hydrogen phosphate and potassium dihydrogen phosphate (pH 5.2–8.0), and (iii) boric acid and sodium hydroxide (pH 7.8–10) by using the prescriptions tabulated by Vogel.[48] In each case the buffer was made 0.1 M in sodium chloride by addition of the required amount of salt, and the pH was measured accurately just before use. A buffer of pH ~4 has been extensively used in the present work. Specific details of the composition of this buffer are as follows: 10.0 mL of 1.0 N sodium acetate, 8.0 mL of 1.0 N hydrochloric acid, and 2.5 mL of 2.0 N sodium chloride were mixed together, and the solution was diluted to 50.0 mL.

Synthesis and Characterization of the Polymer. Commercially available styrene was purified by distillation at reduced pressure and then polymerized in the presence of benzoyl peroxide under a dinitrogen atmosphere. The polystyrene thus obtained was found to have an average molecular weight of 1.05×10^5 from variable-concentration viscometric measurements. It was then sulfonated by hot concentrated sulfuric acid containing silver sulfate catalyst with a reported procedure.[49]

Purified poly(*p*-styrenesulfonic acid) (P-SSH) is completely soluble in water and methanol. The density of the polymer was determined to be 1.33 g/cm^3 by flotation in a mixture of chloroform and benzene. The degree of sulfonation of polystyrene was determined to be 70% by titration with standard sodium hydroxide solution.

The pK of the polymer (~150 mg in 10 mL of aqueous solvent) was determined by pH-metric titration (Type 335 Systronics pH meter) using standard carbonate-free sodium hydroxide solution (0.3239 N) at 298 K. The ionic strength of the polymer solution was varied by using pure water, 0.3 N aqueous NaCl, and 1 N aqueous NaCl as solvent. A sharp end point was observed in all cases, and pK was found to be in the range 1.95 ± 0.05 irrespective of the ionic strength of the polymer solution.

Electrochemistry. (a) Electrodes and Instrumentation. Pyrolytic graphite disks (5.5-mm diameter, 3-mm thickness) were cut from cylindrical stock (Union Carbide Corp., Cleveland, OH) with the basal planes of the graphite perpendicular to the axis of the cylinder. The graphite disks were mounted in a Teflon holder which is a modified version of that reported by Anson et al.[44] The exposed electrode area was determined chronoamperometrically by using a standard aqueous solution of $K_4[Fe(CN)_6]\cdot 3H_2O$ in 0.1 N KCl as the calibrant.[50]

(44) Koval, C. A.; Anson, F. C. *Anal. Chem.* **1978**, *50*, 223.
(45) Abruña, H. D.; Meyer, T. J.; Murray, R. W. *Inorg. Chem.* **1979**, *18*, 3233.
(46) Oyama, N.; Anson, F. C. *Anal. Chem.* **1980**, *52*, 1192.
(47) At low pH, the ion exchange equilibrium in eq 5 may involve H^+ in significant proportions in place of the alkali-metal ion.
(48) Vogel, A. I. "A Text-Book of Quantitative Inorganic Analysis", 2nd ed.; Longmans Green and Co: London, 1951; pp 869–870.
(49) Mukherjee, A. R.; Raha, C. R. *Macromol. Synth.* **1968**, *3*, 140.
(50) Lingane, P. J. *Anal. Chem.* **1964**, *36*, 1723.

Electrochemical measurements were done with the help of a PAR Model 370-4 electrochemistry system incorporating a Model 174A polarographic analyzer, a Model 175 universal programmer, a Model RE 0074 X-Y recorder, a Model 173 potentiostat, a Model 179 digital coulometer, and a Model 377A cell system. A platinum wire and a saturated calomel electrode (SCE) were used as auxiliary and reference electrodes, respectively. Solutions were deaerated with purified dinitrogen and experiments were conducted at 298 K under dinitrogen atmosphere. The potentials are uncorrected for junction contribution.

(b) Procedures. The basal pyrolytic graphite electrodes were freshly cleaved with a razor blade just prior to use. A freshly prepared solution (0.005–0.5 wt %) of P-SSH in 1:1 water–methanol was used for coating. The coating could be achieved in two ways: (i) dipping of electrode into a solution of the polymer for 15 min; (ii) transferring measured aliquots (5 μL) of the polymer solution to the surface of the electrode. In either case the solvent was allowed to evaporate slowly at room temperature. In most experiments reported in this work procedure ii was utilized.

For loading, the coated electrodes were immersed in stirred solutions of $(0.02–1.05) \times 10^{-3}$ M $[NiL](ClO_4)_2$ in the buffer of required pH. Cyclic voltammograms were recorded from time to time till a leveling off of the increased peak current occurred (about 10 min). The electrodes were then removed from the loading solution and briefly rinsed with the same buffer solution without any NiL^{2+}. The electrodes were then carefully dried and finally transferred to pure buffer solution for electrochemical studies.

For determining surface coverage, Γ_{Ni} (i.e. the quantity of NiL^{2+} incorporated by P-SS films per unit area of the electrode), the loaded electrodes were placed in pure buffer and coulometry was performed by holding the potential at values well below the voltammetric peak potential for the reduction of the incorporated NiL^{2+}. Surface coverage was calculated from the relation $\Gamma_{Ni} = Q/nFA$, where n is the number of electrons transferred per molecule reduced, F is Faraday's constant, A is the area of the electrode in cm^2, and Q is the total charge consumed for the reduction of the bound NiL^{2+}. All reported coverage data (corrected for background contributions) are averages of at least three independent measurements. The results are reproducible to within ±20–30%.

The effective concentrations (mol/L) of NiL^{2+} in the P-SS films, $[NiL^{2+}]_p$, were calculated[24] from eq 7 where A is the electrode area and

$$[NiL^{2+}]_p = 10^3 A\Gamma_{Ni}/\beta_p \quad (7)$$

β_p is the volume of polymer film. The value of β_p is calculated from the mass of P-SS in the film, and the polymer film density is taken as roughly equal to the bulk density (1.33 g/cm^3).

The rate constant for the loss of NiL^{2+} from the loaded electrode was calculated from the slope of the semilogarithmic plot of cathodic peak current vs. the time the electrode was exposed to the buffer solution (298 K). The observed rate constant $(3.05 \pm 0.5) \times 10^{-4}$ s^{-1} is the average of four experiments.

Acknowledgment. Financial help received from the Department of Science and Technology, Government of India, New Delhi, India, is gratefully acknowledged. Constructive comments of reviewers were very helpful at the revision stage.

Registry No. $Ni^{II}(H_2L)^{2+}$, 55188-31-3; $Ni^{II}(HL)^+$, 60306-03-8; $Ni^{II}L$, 59980-38-0; $Ni^{III}L^+$, 59980-37-9; $Ni^{IV}L^{2+}$, 55188-33-5; P-SS, 28210-41-5; P-SS (sodium salt), 25704-18-1; graphite, 7782-42-5.

Contribution from the Dipartimento di Chimica Analitica, Università di Torino, 10125 Torino, Italy, and Max-Planck-Institut für Biophysikalische Chemie, 3400 Göttingen, West Germany

Electron-Transfer Kinetics of 4,4′-Bis(alkoxycarbonyl)-2,2′-bipyridine–Iron Complexes in Micellar Solution

Marco Vincenti,† Edmondo Pramauro,† Ezio Pelizzetti,*† Stephan Diekmann,‡ and Jens Frahm‡

Received January 16, 1985

The kinetics of electron-transfer reactions of a series of iron complexes $Fe(EX)_3^{2+}$ (EX = 4,4′-bis(alkoxycarbonyl)-2,2′-bipyridine, with alkoxy = methoxy, ethoxy, propoxy, butoxy) have been studied in homogeneous and in micellar solution. In homogeneous solution the rates of electron-transfer reactions with aquocerium(IV) ions are similar for the different complexes. In the presence of anionic micelles of sodium dodecyl sulfate the observed rate constants are enhanced as compared to those in homogeneous solution. At high surfactant concentrations, the rate enhancement is similar for the different $Fe(EX)_3^{2+}$ complexes investigated, whereas in the region of the critical micelle concentration relevant differences occur. By the use of a theoretical description of the diffuse double layer previously developed, the electrostatic enrichment of counterions at the micellar surface turns out to be the dominating contribution to the overall rate enhancement. If the overall enhancement is divided by the electrostatic part, additional contributions due to alterations of the second-order rate constant in the micellar environment are found. At low surfactant concentrations the results suggest a formation of "micelles" of altered size and shape, which are able to solubilize more than one iron complex. Among these iron complexes charge delocalization effects might occur and further contribute to the rate enhancement.

Introduction

Electron-transfer reactions in organized structures have been extensively investigated in relation to the solar energy conversion[1] and the redox processes in biological systems.[2] Although effects of micelles on electron-transfer rates have received attention, they have been analyzed only in terms of conventional kinetic models.[3] Recently, an attempt has been made to separate the electrostatic from the nonelectrostatic contribution to the apparent overall rate constant. This approach was successfully applied to reactions between aquoions and organic molecules[4] as well as metal complexes with organic ligands.[5] In order to investigate the effect of increasing hydrophobicity on the kinetic properties of metal complexes with organic ligands, the iron complexes $Fe(EX)_3^{2+}$

Chart I

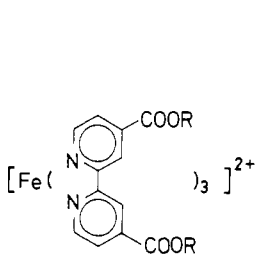

compd	R
$Fe(bpy)_3^{2+}$	
$Fe(EM)_3^{2+}$	CH_3
$Fe(EE)_3^{2+}$	C_2H_5
$Fe(EP)_3^{3+}$	C_3H_7
$Fe(EB)_3^{2+}$	C_4H_9

(EX = 4,4′-bis(alkoxycarbonyl)-2,2′-bipyridine, with alkoxy = methoxy (EM), ethoxy (EE), propoxy (EP), and butoxy (EB))

† Università di Torino.
‡ Max-Planck-Institut für Biophysikalische Chemie.

0020-1669/85/1324-4533$01.50/0